HEAT TRANSFER ENHANCEMENT IN LAMINAR CONVECTIVE HEAT TRANSFER WITH NANOFLUID FLOW IN CIRCULAR CHANNELS

Sadık Kakaç[1], Sezer Özerinç[2], Almıla Güvenç Yazıcıoğlu[3]

Department of Mechanical Engineering

[1]TOBB University of Economics and Technology, sadikkakac@yahoo.com

[2]University of Illinois at Urbana-Champaign, sezerozerinc@hotmail.com

[3]Middle East Technical University, yalmila@metu.edu.tr

ABSTRACT

Accurate prediction of the heat transfer performance of nanofluids is necessary for the utilization of nanofluids in practical applications. The simplest method for the analysis of nanofluid heat transfer is the single-phase approach, where the nanofluid is treated as a single-phase fluid, and the effect of nanoparticles are taken into account only through the usage of the thermophysical properties of the nanofluid in the calculations. In this work, the thermal dispersion model has been utilized through a single-phase, temperature-dependent thermal conductivity approach and the numerical analysis of hydrodynamically fully developed laminar forced convection of Al_2O_3(20 nm)/water nanofluid inside a circular tube under constant wall temperature and constant wall heat flux boundary conditions has been performed. Comparison of numerical results with experimental data indicates good agreement. As a consequence, it is thought that utilizing the thermal dispersion model with single phase assumption is a proper way of analyzing convective heat transfer of nanofluids.

Corresponding author: Dr. Sadık Kakaç

tel. : +90 532 568 1666

fax : +90 312 292 4091

e-mail : sadikkakac@yahoo.com

address : TOBB University of Economics and Technology,

Söğütözü Cad. No: 43, 06560, Ankara, Turkey

HEAT TRANSFER ENHANCEMENT IN LAMINAR CONVECTIVE HEAT TRANSFER WITH NANOFLUID FLOW IN CIRCULAR CHANNELS

Sadık Kakaç[1], Sezer Özerinç[2], Almıla Güvenç Yazıcıoğlu[3]

Department of Mechanical Engineering

[1]TOBB University of Economics and Technology, sadikkakac@yahoo.com

[2]University of Illinois at Urbana-Champaign, sezerozerinc@hotmail.com

[3]Middle East Technical University, yalmila@metu.edu.tr

ABSTRACT

Accurate prediction of the heat transfer performance of nanofluids is necessary for the utilization of nanofluids in practical applications. The simplest method for the analysis of nanofluid heat transfer is the single-phase approach, where the nanofluid is treated as a single-phase fluid, and the effect of nanoparticles are taken into account only through the usage of the thermophysical properties of the nanofluid in the calculations. In this work, the thermal dispersion model has been utilized through a single-phase, temperature-dependent thermal conductivity approach and the numerical analysis of hydrodynamically fully developed laminar forced convection of Al_2O_3(20 nm)/water nanofluid inside a circular tube under constant wall temperature and constant wall heat flux boundary conditions has been performed. Comparison of numerical results with experimental data indicates good agreement. As a consequence, it is thought that utilizing the thermal dispersion model with single phase assumption is a proper way of analyzing convective heat transfer of nanofluids.

Keywords: Nanofluids, heat transfer enhancement, forced convection, laminar flow

INTRODUCTION

With the recent improvements in nanotechnology, the production of particles with sizes on the order of nanometers (nanoparticles) can be done with relative ease. As a consequence, the idea of suspending

these nanoparticles in a base liquid for improving thermal conductivity has been proposed [1,2]. Such suspension of nanoparticles in a base fluid is called a nanofluid. Due to their small size, nanoparticles fluidize easily inside the base fluid, and as a consequence, clogging of channels and erosion in channel walls are no longer a problem. It is even possible to use nanofluids in microchannels [3,4]. When it comes to the stability of the suspension, it was shown that sedimentation of particles can be prevented by utilizing proper dispersants.

Increase in the thermal conductivity of the working fluid improves the efficiency of the heat transfer process. When forced convection in tubes is considered, it is expected that heat transfer coefficient enhancement obtained by using a nanofluid is equal to the enhancement in thermal conductivity of the nanofluid, due to the definition of Nusselt number. However, research about the convective heat transfer of nanofluids indicated that the enhancement of heat transfer coefficient exceeds the thermal conductivity enhancement of nanofluids [5-8]. This extra enhancement indicates the presence of additional heat transfer enhancement mechanisms; such as, particle migration [9] and thermal dispersion [10]. At present, there is controversy about the relative significance of these mechanisms. Therefore, further studies are required for the clarification of the situation.

Accurate prediction of the heat transfer performance of nanofluids is necessary for the utilization of nanofluids in practical applications. There are many studies in the literature regarding the convective heat transfer with nanofluids. The simplest method for the analysis of nanofluid heat transfer is the single-phase approach. In this approach, the nanofluid is treated as a single-phase fluid, and the effect of nanoparticles are taken into account only through the usage of the thermophysical properties of the nanofluid in the associated calculations. A numerical study that follows this approach was performed by Maïga et al. [11] by considering the laminar and turbulent flow of Al_2O_3/water and Al_2O_3/ethylene glycol nanofluids inside a straight circular tube under constant wall heat flux boundary condition. The study showed that ethylene glycol-based nanofluids provide better heat transfer enhancement when compared to the water-based nanofluids.

The single-phase approach can be modified by utilizing a thermal dispersion model proposed by Xuan and Roetzel [10]. The model takes the effect of improved thermal transport due to the random motion of nanoparticles into account. Heris et al. [12] performed a numerical study based on the thermal dispersion model [10] by considering the laminar flow of Al_2O_3/water nanofluid inside a straight circular tube under constant wall temperature boundary condition. The researchers concluded that the heat transfer enhancement obtained with nanofluids increases with decreasing particle size and increasing particle volume fraction.

Nanofluid flow can also be investigated by utilizing a two-phase approach. Bianco et al. [13] performed such an analysis by modeling the force interactions between nanoparticles and the fluid matrix. Similar to the previously mentioned studies, laminar flow of Al_2O_3/water nanofluid inside a straight circular tube was considered under constant wall heat flux boundary condition. The analysis was repeated by using the single-phase approach, and it was concluded that the single-phase analysis provides close results to those of the two-phase approach as long as the variation of nanofluid thermophysical properties with temperature is taken into account.

ANALYSIS

In this analysis, the thermal dispersion model is investigated through the utilization of numerical methods. Therefore, a numerical analysis of convective heat transfer of laminar Al_2O_3/water nanofluid flow inside a straight circular tube with temperature-dependent thermal conductivity and thermal dispersion has been performed.

Flow Configuration

In the numerical study, forced convection heat transfer performance of Al_2O_3/water nanofluid in the laminar flow regime in a straight circular tube is analyzed. Velocity profile is fully developed and the flow is considered as incompressible. The boundary conditions analyzed are constant wall temperature and constant wall heat flux. Such a flow condition is common in practical applications in which the flow becomes hydrodynamically fully developed in an unheated entrance region. A schematic view of the flow configuration is provided in Fig. 1.

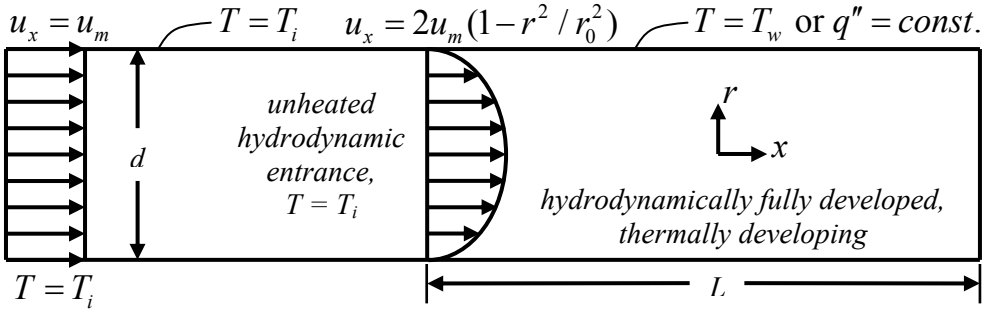

Fig. 1. Schematic representation of the flow configuration for the numerical analysis

Nanofluid Modeling

In the present analysis, the nanofluid is considered as a single phase fluid. Such an approach is a more practical way of analyzing heat transfer of nanofluids. However, the validity of the single phase assumption needs verification. It should be noted that solely substituting the thermophysical properties of the nanofluid to the governing equations is not much different than using the classical correlations of convective heat transfer with thermophysical properties of the nanofluid, which has been shown to underestimate the experimental results [14]. Therefore, the single phase analysis requires some modifications in order to account for the additional enhancement. For this purpose, the thermal dispersion model proposed by Xuan and Roetzel [10] is used.

Xuan and Roetzel [10] noted that thermal dispersion occurs in nanofluid flow due to the random motion of nanoparticles. By considering the fact that the random motion of the particles creates small perturbations in velocity and temperature, they showed that the effective thermal conductivity in the energy equation takes the following form.

$$k_{eff} = k_{nf} + k_d \tag{1}$$

Here, k_{nf} is nanofluid thermal conductivity. Variation of thermophysical properties with temperature is an important issue for the modeling of nanofluid flow. Experimental studies show that especially thermal conductivity of nanofluids significantly changes with temperature. As a consequence, constant thermal conductivity assumption in the numerical analysis may lead to erroneous results. Therefore, in the present analysis, variation of thermal conductivity with temperature is taken into account. For this purpose, a temperature dependent empirical correlation proposed by Chon et al. [15] is used due to its

wide range of applicability and relatively good agreement with experimental data. With this model, k_{nf} may be determined with the following expression.

$$\frac{k_{nf}}{k_f} = 1 + 64.7\phi^{0.7460}\left(\frac{d_f}{d_p}\right)^{0.3690}\left(\frac{k_p}{k_f}\right)^{0.7476}\mathrm{Pr}^{0.9955}\,\mathrm{Re}^{1.2321} \tag{2}$$

Here, d_f is the diameter of the fluid molecules. Prandtl number and Reynolds number are defined as follows.

$$\mathrm{Pr} = \frac{\mu_f}{\rho_f \alpha_f} \tag{3}$$

$$\mathrm{Re} = \frac{\rho_f V_{Br} d_p}{\mu_f} \tag{4}$$

α_f is the thermal diffusivity of the base fluid. V_{Br} is the Brownian velocity of the nanoparticles and it is calculated by using the following expression.

$$V_{Br} = \frac{\kappa_B T}{3\pi\mu_f d_p \lambda_f} \tag{5}$$

κ_B is Boltzmann constant and T is temperature in K. λ_f is mean-free path of the fluid molecules, and it is 0.17 nm for water. The validity range of the correlation is between 11 nm and 150 nm for particle diameter, 1% and 4% for particle volume fraction, and 21°C and 71°C for temperature.

In Eq. (1) k_d is dispersed thermal conductivity and it was proposed that it can be calculated by using the following expression [10].

$$k_d = C(\rho c_p)_{nf} u_x \phi d_p r_0 \tag{6}$$

ρ is density, c_p is specific heat, u_x is axial velocity, ϕ is particle volume fraction, d_p is nanoparticle diameter, and r_0 is tube radius. C is an empirical constant that should be determined by matching experimental data. Eqs. (5,6) are used in the present analysis for both axial and radial thermal

conduction terms and the variation of dispersed thermal conductivity in radial direction due to the variation of axial velocity in radial direction is taken into account.

In the present analysis, for the determination of nanofluid density and specific heat, Eqs. (7) and (8) are used, respectively.

$$\rho_{nf} = \phi\rho_p + (1-\phi)\rho_f \tag{7}$$

$$(\rho c_p)_{nf} = \phi(\rho c_p)_p + (1-\phi)(\rho c_p)_f \tag{8}$$

For viscosity, an empirical correlation proposed by Nguyen et al. [16] for Al_2O_3/water nanofluids is used:

$$\mu_{nf} = (1 + 2.5\phi + 150\phi^2)\mu_f \tag{9}$$

The above correlation is valid for the nanofluids with a particle size of 36 nm. Experimental studies show that particle size is an important parameter that affects the viscosity of nanofluids. However, at present, it is difficult to obtain a consistent set of experimental data for nanofluids that covers a wide range of particle size and particle volume fraction. Therefore, for the time being, Eq. (9) can be used as an approximation for Al_2O_3/water nanofluids with different particle sizes. When it comes to temperature dependence of viscosity, Nguyen et al. [16] showed that for particle volume fractions below 4%, viscosity enhancement ratio (viscosity of nanofluid divided by the viscosity of base fluid) does not significantly change with temperature.

Formulation of the Problem

The single-phase thermal dispersion approach described in the previous section does not modify the governing equations of continuity and momentum for pure fluids except for the nanofluid thermophysical properties used in the associated expressions. As a consequence, the fully developed axial velocity profile of the nanofluid flow can be obtained as

$$u_x = 2u_m\left(1 - \frac{r^2}{r_0^2}\right), \tag{10}$$

where r is radial position and u_m is the mean velocity. Under the assumptions stated, the general energy equation reduces to [17]

$$(\rho c_p)_{nf}\left[\frac{\partial T}{\partial t}+2u_m\left(1-\frac{r^2}{r_0^2}\right)\frac{\partial T}{\partial x}\right]=\frac{1}{r}\frac{\partial}{\partial r}\left(k_{eff}\,r\frac{\partial T}{\partial r}\right)+\frac{\partial}{\partial x}\left(k_{eff}\frac{\partial T}{\partial x}\right) \tag{11}$$

Here, according to the thermal dispersion model, the thermal conductivity term is replaced by the effective thermal conductivity (k_{eff}), which is not a constant and it varies in x- and r-directions. Viscous dissipation has been neglected, because the Brinkman number that defines the significance of viscous effects in the flow is determined to be on the order of 10^{-7}. The term with time derivative is conserved in Eq. (11) due to the fact that the utilized numerical solution reaches the steady-state solution by progressing in time. The following two sections discuss the subsequent steps of the analysis regarding the problem formulation depending on the boundary condition. Section 3.3.3 describes the determination of the heat transfer coefficient and Nusselt number.

Constant Wall Temperature Boundary Condition

For constant wall temperature boundary condition, the following nondimensional parameters are defined.

$$\theta=\frac{T-T_w}{T_i-T_w},\quad x^*=\frac{x}{r_0},\quad r^*=\frac{r}{r_0},\quad t^*=\frac{\alpha_{nf,b}t}{r_0^2},\quad k^*=\frac{k_{eff,T}}{k_{nf,b}},\quad Pe_{nf}=\frac{u_m d}{\alpha_{nf,b}}, \tag{12-17}$$

where T_i and T_w are inlet and wall temperatures, respectively. In the thermal conductivity expression, subscript T indicates that the effective thermal conductivity should be calculated at local temperature, whereas subscript b corresponds to the bulk mean temperature. $k_{eff,T}$ is calculated according to Eqs. (1, 2, 6). Using Eqs. (12-17), the nondimensional form of Eq. (11) becomes the following:

$$\frac{\partial\theta}{\partial t^*}+Pe_{nf}\left(1-r^{*2}\right)\frac{\partial\theta}{\partial x^*}=\frac{1}{r^*}\frac{\partial}{\partial r^*}\left(k^*r^*\frac{\partial\theta}{\partial r^*}\right)+\frac{\partial}{\partial x^*}\left(k^*\frac{\partial\theta}{\partial x^*}\right) \tag{18}$$

Eq. (18) is the final form of the energy equation that is numerically solved. The nondimensional boundary conditions are as follows.

$$\frac{\partial \theta}{\partial r^*} = 0 \text{ at } r^* = 0, \ \theta = 0 \text{ at } r^* = 1, \ \theta = 1 \text{ at } x^* = 0. \tag{19-21}$$

Constant Wall Heat Flux Boundary Condition

For constant wall heat flux boundary condition, nondimensional parameters are the same as the expressions provided for constant wall temperature boundary condition (Eqs. 12-17), except the definition of the nondimensional temperature, θ.

$$\theta = \frac{k_{nf}\left(T - T_i\right)}{q_w'' r_0}, \tag{22}$$

where q_w'' is the wall heat flux, and r_0 is tube radius. Resulting nondimensional energy equation is the same as the expression provided in Eq. (18). The boundary conditions are

$$\frac{\partial \theta}{\partial r^*} = 0 \text{ at } r^* = 0, \ \frac{\partial \theta}{\partial r^*} = \frac{1}{k^*} \text{ at } r^* = 1, \ \theta = 0 \text{ at } x^* = 0. \tag{23-25}$$

Determination of Heat Transfer Coefficient and Nusselt Number

After the determination of the temperature distribution in the flow domain through the numerical solution of Eq. (18), local heat transfer coefficient can be determined by using the following expression.

$$h_{nf,x} = \frac{k_{eff,w,x}\left(\frac{\partial T}{\partial r}\right)_{x,r_0}}{T_{w,x} - T_{m,x}}, \tag{26}$$

where $T_{m,x}$ and $T_{w,x}$ are mean temperature and wall temperature at axial location x, respectively. $T_{m,x}$ can be determined by calculating the following expression numerically.

$$T_{m,x} = \frac{\int_0^{r_0} 2ru_x(x,r)T(x,r)dr}{u_m r_0^2} \tag{27}$$

$k_{eff,w,x}$ is the effective thermal conductivity at the wall, and $(\partial T / \partial r)$ is calculated by using a finite difference formulation. Nusselt number is determined as follows.

$$Nu_x = \frac{h_x d}{k_{eff,w,x}} . \quad (28)$$

Average values of the heat transfer coefficient and Nusselt number are determined by integrating the local values along the tube and dividing the result by the tube length.

Numerical Methodology

In the numerical solution, finite difference method is utilized by using C programming language. In Eq. (18), all of the terms are discretized by second order differencing. In order to ensure stability, backward differencing is used for the convection term (second term on the left-hand side of Eq. 18). For other terms, central differencing is used. As the solution scheme, Alternating Direction Implicit (ADI) scheme is used [18]. ADI scheme consists of two time steps that are repeated iteratively. In the first time step, discretization is made such that the discretizations in *x*-coordinate are implicit and the discretizations in *y*-coordinate are explicit. In the second time step, the discretizations in *x*-coordinate are explicit and the discretizations in *y*-coordinate are implicit. These two steps are repeated iteratively to obtain the transient solution of the problem. In the present analysis, the objective is to obtain the steady-state solution of the problem. Therefore, in the solution, time steps are selected to be large and solution is progressed in time until the variation of temperature distribution with time becomes negligible.

One of the most important solution parameters is the number of nodes used in the solution. For determining proper values, numerical results obtained by utilizing 400x100, 200x50, 100x25, and 50x12 grids are compared in terms of the variation of local Nusselt number in axial direction (first numbers are the number of nodes in *x*-direction whereas second numbers indicate the number of nodes in *r*-direction). As a result of the comparison, it is determined that for the constant wall temperature boundary condition, 200x50 grid is sufficient for the accurate analysis of the problem; whereas 100x25 grid is sufficient for the accurate analysis of the constant wall heat flux case.

Code Verification

The consistency of the numerical solution is shown by the grid independence analysis presented in the previous section. However, the numerical results should also be theoretically examined for ensuring the validity of the analysis. For that purpose, numerical results are compared with the results of Graetz solution [19] for parabolic velocity profile for both of the boundary conditions. As explained in detail elsewhere [14], there is perfect agreement between the Graetz solution and the current results for water.

RESULTS

Constant Wall Temperature Boundary Condition

In this section, first, the results of the numerical analysis are compared with experimental and numerical data available in the literature. Then, a further analysis is presented for the local Nusselt number, the effect of particle diameter, and the effects of heating and cooling in the nanofluid flow.

In Fig. 1, a comparison of the current results with and without thermal dispersion are provided, with experimental and numerical results in literature for the variation of average heat transfer coefficient enhancement ratio with Peclet number. For this pupose, the studies of Heris et al [7,12] are selected. Heris et al. investigated the heat transfer performance of Al_2O_3(20 nm)/water nanofluids both experimentally [7] and numerically – based on the experimental results [12]. In their experiments [7], the test section is a straight circular tube with a diameter of 5 mm and length of 1 m, particle volume fraction was varied between 0.2% and 2.5% and Peclet number was varied between 2500 and 6500. The same parameters are used in the current analysis. In order to focus on the sole effect of the nanofluid thermophysical properties and thermal dispersion on heat transfer, the enhancement values are calculated by considering the results of the nanofluid and pure water for the same Peclet number. In order not to overcrowd Fig. 1, only the data for $\phi = 1$ % and $\phi = 2$ % are presented therein.

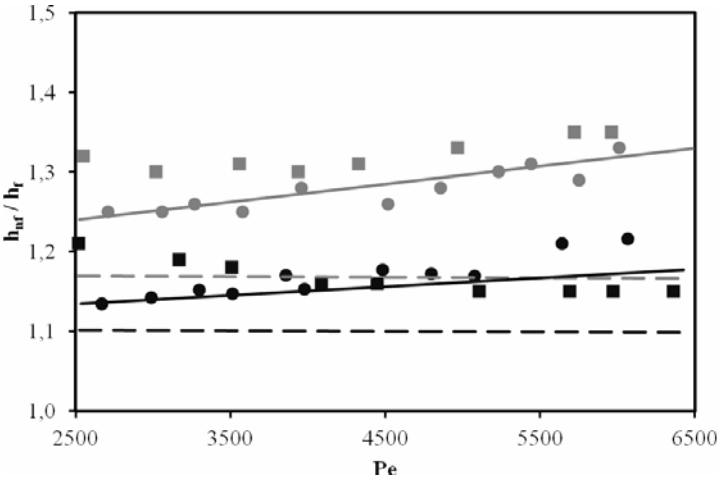

Fig. 2. Comparison of the numerical results with experimental and numerical data of Heris et al. [7,12] for constant wall temperature. Solid and dashed lines indicate the numerical solution with and without thermal dispersion, respectively. Circles and squares indicate the experimental [7] and numerical [12] results of Heris et al. All data in black are for ϕ = 1 % and in gray are for ϕ = 2 %. *Pe* is Pe_{nf} for nanofluid and Pe_f for base fluid.

When Fig. 1 is examined, it can be observed that the analysis performed by neglecting the thermal dispersion significantly underpredicts the experimental data. On the other hand, the numerical results with thermal dispersion correctly predict the experimental data [7]; there is a slight increase in the enhancement values with increasing Peclet number. When numerical data of Heris et al. [12] are considered, a significant discrepancy may be observed. The main reason for this may be the use of constant nanofluid thermal conductivity and constant dispersed thermal conductivity in their work, whereas in the current work, variation of these parameters with temperature and radial position are taken into account, respectively. Since the numerical results of the current study are in complete agreement with the experimental data of Heris et al. [7], it can be concluded that taking the variation of thermal conductivity and thermal dispersion into account improves the accuracy of the numerical solution significantly.

Local Nusselt Number

In order to determine the fully developed Nusselt number as well, the flow inside a longer tube is considered (5 m). Figure 3 shows the results for the flow of pure water and Al_2O_3/water nanofluid at a Peclet number of 6500. In the figure, it is seen that the local Nusselt number is larger for nanofluids throughout the tube. This is mainly due to the thermal dispersion in the flow. Thermal dispersion results in a higher effective thermal conductivity at the center of the tube which flattens the radial temperature profile. Flattening of temperature profile increases the temperature gradient at the tube

wall and as a consequence, Nusselt number becomes higher when compared to the flow of pure water. Figure 3 also shows that increasing particle volume fraction increases Nusselt number. This is due to the fact that the effect of thermal dispersion becomes more pronounced with increasing particle volume fraction.

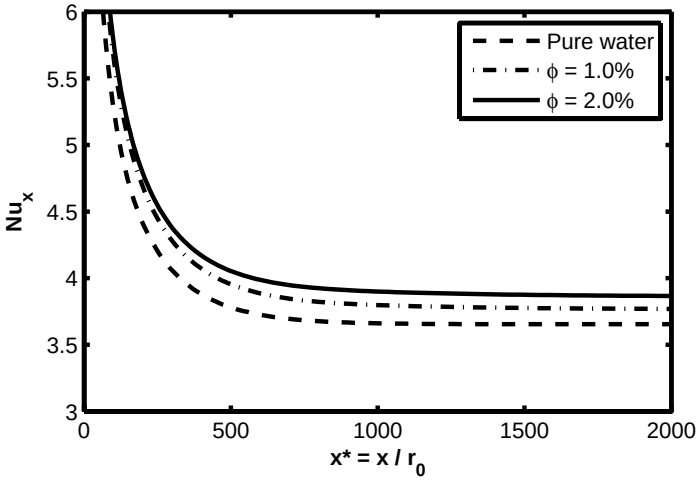

Fig. 3. Variation of local Nusselt number with dimensionless axial position for pure water and Al_2O_3/water nanofluid, $Pe_{nf} = Pe_f = 6500$

Effect of Particle Diameter

Most of the experimental data in the literature indicates increasing thermal conductivity with decreasing particle size. On the other hand, decreasing particle size decreases the effect of thermal dispersion through Eq. (6). In order to understand the relative significance of these effects, average heat transfer coefficient enhancement ratio is plotted in Fig. 4 with respect to Peclet number for 1 vol.% Al_2O_3/water nanofluids with different particle sizes. The flow configuration in consideration is the same as the one utilized in the previous sections.

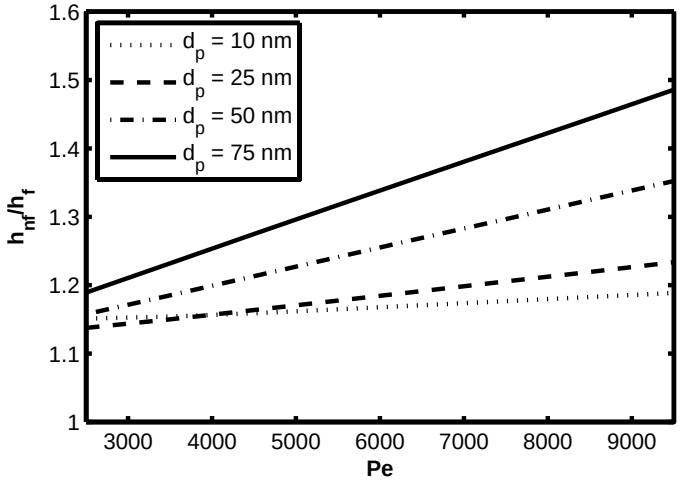

Fig. 4. Variation of average heat transfer coefficient enhancement ratio with Peclet number for different particle sizes of the 1 vol.% Al_2O_3/water nanofluid

When Fig. 4 is examined, it is seen that heat transfer coefficient enhancement ratio generally increases with increasing particle size, which shows that particle size dependence of thermal dispersion is more pronounced than the associated dependence of thermal conductivity. There is an exception for particle sizes below 25 nm at low Peclet number values, therefore variation of thermal conductivity with particle size is more effective for those cases.

Effects of Heating and Cooling

Thermal conductivity distribution of the working fluid inside the tube is an important parameter in heat transfer. Especially, thermal conductivity at the wall significantly affects heat transfer. Since thermal conductivity of nanofluids is a strong function of temperature, heat transfer performance of nanofluids depends on whether the working fluid is heated or cooled. Thermal conductivity of nanofluids increases with temperature, and as a consequence, convective heat transfer coefficient and associated enhancement ratio are larger for the heating of the nanofluid in which T_w has a higher value.

In Fig. 5, this difference is illustrated in terms of the variation of average heat transfer coefficient enhancement ratio with Peclet number for heating and cooling of 2.0 vol.% Al_2O_3/water nanofluid. The flow configuration in consideration is the same as the one utilized in the previous sections. For heating case, T_i = 20°C, and T_w = 65°C whereas for cooling T_i = 65°C, and T_w = 20°C. It is seen that the enhancement difference between the two cases exceeds 5% at low Peclet numbers. Increasing the difference between inlet and wall temperatures, and increasing the particle volume fraction of the nanofluid might result in larger differences in enhancement values.

The results presented in this section show that nanofluids provide higher heat transfer enhancement in heating applications when compared to cooling cases. This fact should be taken into account for the proper design of heat transfer processes with nanofluids.

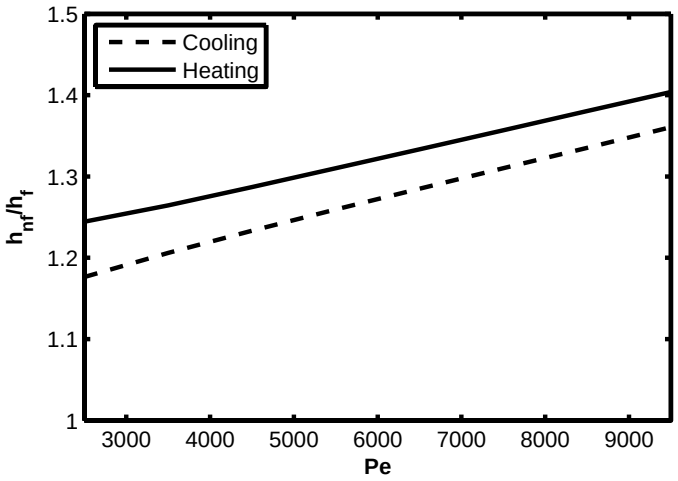

Fig. 5. Variation of average heat transfer coefficient enhancement ratio with Peclet number for heating and cooling of the 2 vol.% Al_2O_3/water nanofluid

Constant Wall Heat Flux Boundary Condition

In this section, an analysis similar to the constant wall temperature boundary condition is presented. First, the results of the numerical analysis are compared with experimental and numerical data available in the literature. Then, a further analysis is presented for the local Nusselt number, the effect of particle diameter, and the effects of heating and cooling in the nanofluid flow.

In Fig 6, a comparison of the current results with the experimental data of Kim et al. [20] are presented for the variation of the local heat transfer coefficient with axial position, for water and nanofluid. Kim et al. considered the laminar flow of 3 vol.% Al_2O_3/water nanofluid inside a straight circular tube. Test section has a length of 2 m and diameter of 4.57 mm. Inlet temperature of the flow is 22°C, and a 60 W source is used for obtaining a constant wall heat flux boundary condition. Al_2O_3 particles used in the study have a size distribution of 20 – 50 nm. The same parameters are used in the current work. As can be observed in Fig. 6, the numerical results and experimental data are in complete agreement for both the nanofluid flow and pure water flow.

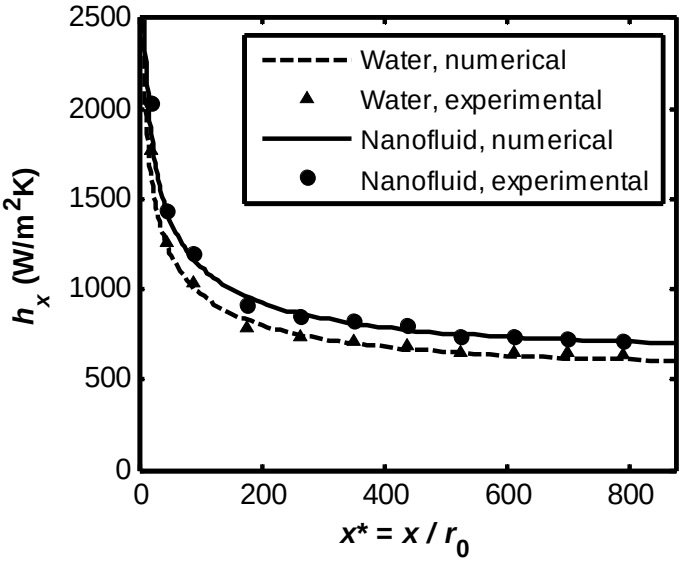

Fig. 6. Comparison of the numerical results with experimental data of Kim et al. [20] for the constant wall heat flux boundary condition. Lines and markers indicate numerical results and experimental data, respectively. $Re_{nf} = Re_f = 1460$

Local Nusselt Number

In this section, the same flow configuration analyzed numerically in the previous sections (test section of Kim et al. [20] is investigated in terms of the axial variation of local Nusselt number. Figure 7 shows the results for the flow of pure water and Al_2O_3/water nanofluid at a Peclet number of 12000 ($Re \approx 2000$). In the figure, it is seen that the local Nusselt number is larger for nanofluids throughout the tube, similar to the case of constant wall temperature boundary condition. However, the difference between the nanofluid Nusselt number and pure water Nusselt number is smaller when compared to constant wall temperature boundary condition. This is mainly due to the fact that the utilized empirical constant C (Eq. 6) is smaller for the present case when compared to constant wall temperature case, which is selected to be so in order to match the experimental data of Kim et al. [20].

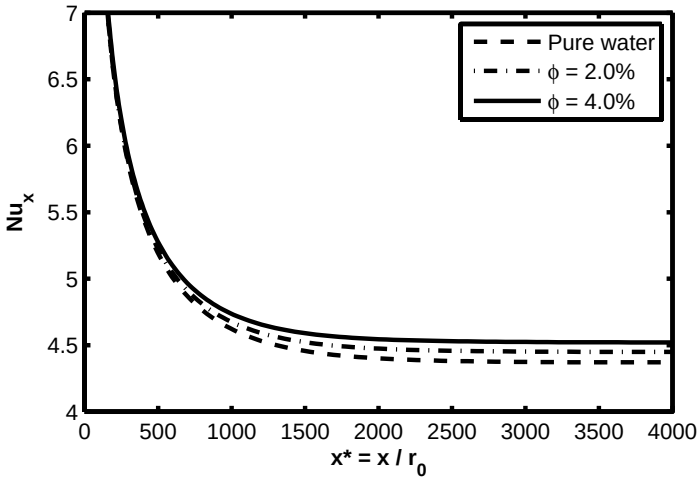

Fig. 7. Variation of local Nusselt number with dimensionless axial position for pure water and Al_2O_3/water nanofluid, $Pe_{nf} = Pe_f = 12000$

Effect of Particle Diameter

An analysis similar to the constant wall temperature boundary condition is performed in this section for the constant wall heat flux boundary condition. In the analysis, the flow configuration and associated parameters are the same as the ones utilized in the previous section. Numerical results are presented in Fig. 8 in terms of the variation of local heat transfer coefficient with axial direction. In the figure, Pe = 2500 and 4 vol.% Al_2O_3/water nanofluid is considered.

When the figure is examined, it is seen that heat transfer coefficient increases with decreasing particle diameter. This is mainly due to the fact that the particle size dependence of thermal conductivity is more pronounced than the particle size dependence of thermal dispersion due to the relatively low empirical constant C used in Eq. (6). In constant wall temperature case, C was chosen to be higher to match experimental data and thermal dispersion dominated the particle size dependence of heat transfer as a consequence. This resulted in increasing enhancement with increasing particle size in constant wall temperature case. For higher values of Peclet number, a similar trend can also be observed for the constant wall heat flux boundary condition.

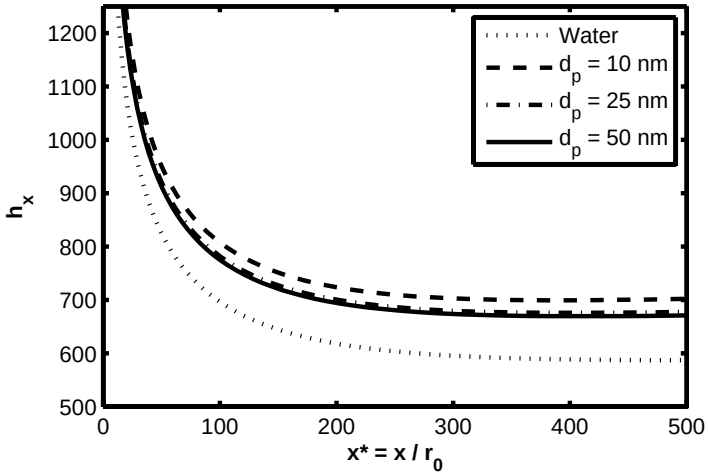

Fig. 8. Variation of local heat transfer coefficient with dimensionless axial position for different particle sizes of 4 vol.% Al_2O_3/water nanofluid

Effects of Heating and Cooling

Effects of heating and cooling on heat transfer enhancement are previously discussed for the case of constant wall temperature boundary condition. In that case, heating of the working fluid provided higher enhancement since thermal conductivity of the working fluid at the wall significantly affects

the heat transfer. When it comes to the constant wall heat flux, the analysis is performed by firstly considering the heating case according to the parameters in the previous section and exit temperature is determined (62°C). For the cooling case, that exit temperature is substituted as inlet temperature and the direction of the heat flux at the wall is reversed. As a consequence, exit temperature of the cooling case (22°C) is equal to the inlet temperature of the heating case.

The results for these two cases are presented in terms of the variation of local heat transfer coefficient with axial direction in Fig. 9. 4 vol.% Al_2O_3/water nanofluid is considered and the results for the flow of pure water are also presented for comparison purposes.

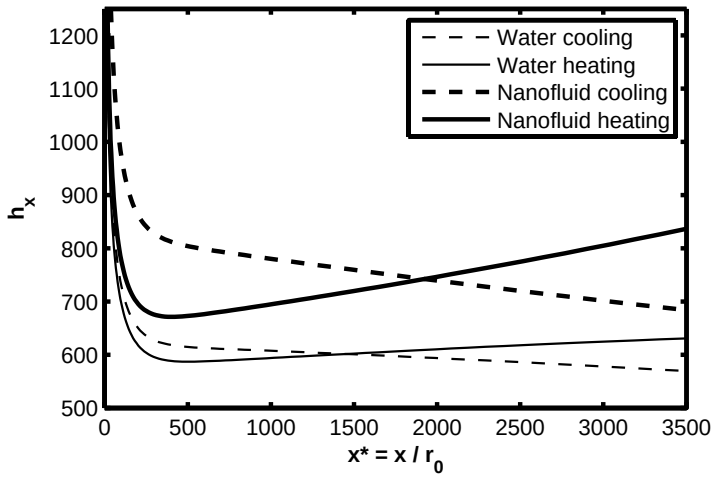

Fig. 9. Variation of local heat transfer coefficient with dimensionless axial position for heating and cooling of the 4 vol.% Al_2O_3/water nanofluid and pure water

It is seen that for both the nanofluid and pure water, heat transfer coefficient is higher for the cooling case at the beginning since the temperature of the fluid is higher in this region when compared to the heating case. At larger values of axial position, the heating case has higher heat transfer coefficient since the temperature of the flow exceeds the corresponding temperature of the cooling case. The important issue here is that the difference between the cooling and heating cases for the nanofluid is much higher than the difference for the pure water.

CONCLUSIONS

In order to examine the validity of the thermal dispersion approach, a numerical analysis of forced convection heat transfer of nanofluids is performed. Comparison of numerical results with experimental data indicates good agreement. As a consequence, it is thought that utilizing the thermal

dispersion model with single phase assumption is a proper way of analyzing convective heat transfer of nanofluids. It should also be noted that this approach requires less computational effort when compared to two-phase analysis, which is important for practical applications.

In constant wall temperature case, the importance of taking the variation of thermal conductivity and thermal dispersion into account in nanofluid heat transfer analysis is emphasized by comparing the results of the present numerical study with another numerical study which assumes constant values for the associated parameters. When it comes to constant wall heat flux case, present numerical results are compared with an available experimental study and complete agreement is observed.

Examination of local Nusselt number of nanofluids revealed that thermal dispersion enhances Nusselt number, which can be explained by the flattening in the radial temperature profile. In addition, heat transfer performance is significantly more dependent on temperature when compared to pure fluids. This fact should be taken into account for the proper design of heat transfer processes with nanofluids.

Further verification of the accuracy of the thermal dispersion model requires more systematic experimental studies, such as the investigation of the effect of particle size and tube diameter on convective heat transfer. In addition, thermal conductivity of nanofluids is a key issue for the proper analysis of convective heat transfer of nanofluids. Therefore, further experimental and theoretical research in that area is also needed for more reliable analyses of the problem.

ACKNOWLEDGEMENTS

The authors wish to thank the Scientific and Technological Research Council of Turkey (TUBITAK) for financial support.

NOTATION

c_p – specific heat capacity, J/kgK; d – tube diameter, m; d_p – nanoparticle diameter, m; h – average heat transfer coefficient, W/m^{2}K; k – thermal conductivity, W/mK; Nu – average Nusselt

number, hd / k; Pe – Peclet number, ud / α; Pr – Prandtl number, ν / α; q'' – heat flux, W/m^2; r – radius, m; r_0 – tube radius, m; Re – Reynolds number, ud / ν; T – temperature, K; u_m – mean flow velocity, m/s; u_x – axial flow velocity, m/s; α – thermal diffusivity, m^2/s; θ – dimensionless temperature; κ_B – Boltzmann constant, 1.3807×10^{-23} J/K; μ – dynamic viscosity, Pa·s; ν – kinematic viscosity, m^2/s; ρ – density, kg/m^3; ϕ – particle volume fraction; **Subscripts:** b – bulk mean; d – dispersed; *eff* – effective; f – base fluid; *fd* – fully developed; i – inlet; *nf* – nanofluid; o – outlet; p – nanoparticle; w – wall; x – local.

REFERENCES

[1] Masuda H., Ebata A., Teramae K., et al. Alteration of thermal conductivity and viscosity of liquid by dispersing ultra-fine particles (dispersion of γ-Al2O3, SiO_2, and TiO_2 ultra-fine particles) // Netsu Bussei. 1993. Vol. 4, No. 4. Pp. 227-233.

[2] Choi S. U. S. Enhancing thermal conductivity of fluids with nanoparticles // American Society of Mechanical Engineers, Fluids Engineering Division (Publication) FED. 1995. Pp. 99-105.

[3] Chein R., and Chuang J. Experimental microchannel heat sink performance studies using nanofluids // Int. J. Therm. Sci. 2007. Vol. 46, No. 1. Pp. 57-66.

[4] Lee J. and Mudawar I. Assessment of the effectiveness of nanofluids for single-phase and two-phase heat transfer in micro-channels // Int. J. Heat Mass Tran. 2007. Vol. 50, No. 3-4. Pp. 452-463.

[5] Pak B. C., and Cho Y. I.Hydrodynamic and heat transfer study of dispersed fluids with submicron metallic oxide particles // Exp. Heat Transfer. 1998. Vol. 11, No. 2. Pp. 151-170.

[6] Hwang K. S., Jang S. P., and Choi S. U. Flow and convective heat transfer characteristics of water-based Al_2O_3 nanofluids in fully developed laminar flow regime // Int. J. Heat Mass Tran. 2009. Vol. 52, No. 1-2. Pp. 193-199.

[7] Heris S. Z., Esfahany M. N., and Etemad S. Experimental investigation of convective heat transfer of Al2O3/water nanofluid in circular tube // Int. J. Heat Fluid Fl. 2007. Vol. 28, No. 2. Pp. 203-210.

[8] Heris S. Z., Etemad S., and Esfahany M. N. Experimental investigation of oxide nanofluids laminar flow convective heat transfer // Int. Commun. Heat Mass. 2006. Vol. 33, No. 4. Pp. 529-535.

[9] Ding Y., and Wen D. Particle migration in a flow of nanoparticle suspensions // Powder Technol. 2005. Vol 149. No. 2-3. Pp. 84-92.

[10] Xuan Y., and Roetzel W. Conceptions for heat transfer correlation of nanofluids // Int. J. Heat Mass Tran. 2000. Vol. 43, No. 19. Pp. 3701-3707.

[11] Maïga S. E. B., Nguyen C. T., Galanis N. et al. Heat transfer behaviours of nanofluids in a uniformly heated tube // Superlattices and Microstructures. 2004. Vol. 35, No. 3-6. Pp. 543-557.

[12] Heris S. Z., Esfahany M. N., and Etemad G. Numerical investigation of nanofluid laminar convective heat transfer through a circular tube // Numer. Heat Tr. A-Appl. 2007. Vol. 52, No. 11. Pp. 1043-1058.

[13] Bianco V., Chiacchio F., Manca O. et al. Numerical investigation of nanofluids forced convection in circular tubes // Appl. Therm. Eng. 2009. Vol. 29, No. 17-18. Pp. 3632-3642.

[14] Özerinç S. Heat transfer enhancement with nanofluids // M.Sc. Thesis, Middle East Technical University, Ankara, Turkey. 2010.

[15] Chon C. H., Kihm K. D., Lee S. P. et al. Empirical correlation finding the role of temperature and particle size for nanofluid (Al_2O_3) thermal conductivity enhancement // Appl. Phys. Lett. 2005. Vol. 87, No. 15. P. 153107.

[16] Nguyen C., Desgranges F., Roy G., et al. Temperature and particle-size dependent viscosity data for water-based nanofluids - Hysteresis phenomenon // Int. J. Heat Fluid Fl. 2007. Vol. 28, No. 6. Pp. 1492-1506.

[17] Kakaç S., and Yener Y. Convective Heat Transfer: Second Edition. CRC-Press: Boca Raton, 1995.

[18] Özışık M. N. Finite Difference Methods in Heat Transfer. CRC-Press: Boca Raton, 1994.

[19] Graetz L. Über die Wärmeleitungs fähigkeit von Flüssigkeiten // Ann. Phys. Chem. 1883. Vol.

18. Pp. 79-94.

[20] Kim D., Kwon Y., Cho Y., et al. Convective heat transfer characteristics of nanofluids under laminar and turbulent flow conditions // Current Applied Physics. 2009. Vol. 9, No. 2, Supplement 1. Pp. e119-e123.